PROCEEDINGS A

rspa.royalsocietypublishing.org

Research

Article submitted to journal

Subject Areas:
Applied Mathematics, Biomechanics, Mechanics

Keywords:
Instabilities, Kirchhoff Rods, Variational Problems, Elasticity, Capillary Adhesion

Author for correspondence:
Insert corresponding author name
e-mail: gaetano.napoli@unisalento.it

THE ROYAL SOCIETY
PUBLISHING

A Tale of Two Nested Elastic Rings

G. Napoli [1] and A. Goriely[2]

[1]Dipartimento di Matematica e Fisica 'E. De Giorgi', Università del Salento, Italy
[2]Mathematical Institute, University of Oxford, UK

Elastic rods in contact provide a rich paradigm for understanding shape and deformation in interacting elastic bodies. Here, we consider the problem of determining the static solutions of two nested elastic rings in the plane. If the inner ring is longer than the outer ring, it will buckle creating a space between the two rings. This deformation can be further influenced by either adhesion between the rings or if pressure is applied externally or internally. We obtain an exact solution of this problem when both rings are assumed inextensible and unshearable. Through a variational formulation of the problem, we identify the boundary conditions at the contact point and use the Kirchhoff analogy to give exact solutions of the problems in terms of elliptic functions. The role of both adhesion and pressure is explored.

1. Introduction

We start with a simple experiment. We take two elastic rings of different sizes and we insert the larger one inside the smaller one. Assuming that the rings are nearly inextensible, the larger ring must buckle to fit inside the smaller one, creating a *blister* as seen in Fig. 1. We also observe that the smaller ring deforms since non-uniform pressure is exerted on its walls. We are naturally led to the following questions: what is the shape of this blister? How does it depend on the geometric and material parameters of the problem?

This type of inner blister is observed in the problem of arterial dissection [1] a small tear forms in the innermost lining of the arterial wall. Since blood is able to enter the blister space between the two layers, a difference in pressure is created between the two spaces, potentially causing narrowing or complete occlusion [2]. The problem of the two elastic rings in the plane is a simple toy model of this process for which the respective role of adhesion, relative stiffness and length, and differential pressure can be studied in details.

This problem is also the simplest problem for the study of interacting elastic bodies in large deformations. While the interaction of a single elastic rings inside a hard ring has been studied extensively [3–6] as a paradigm for elastic materials under confinment [7], the problem of two interacting elastic rods has received little attention (see however, the interesting early work on the self-interaction of a rod in the plane [8] and recent work on self-encapsulation [9]).

Here, we model the two rings as inextensible and unshearable Kirchhoff closed elastic rods. These rods are touching each other and allowed to deform in the plane. The rods are subjected to a pressure due to either external pressure or internal pressures (inside the smaller ring and/or between the ring). In particular an increase in pressure between the ring will naturally tend to increase the size of the blister. We formulate the problem using a variational approach that easily captures the bulk equations as well as the boundary conditions associated with a free boundary (at the point of first contact between the rings) and focus our analysis on symmetric configurations.

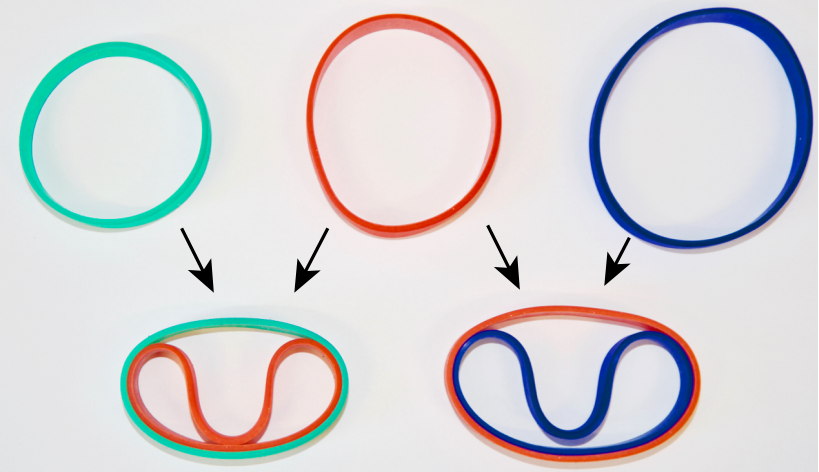

Figure 1. Initially circular silicon bands are inserted into a smaller ring creating a deformed ring with a well-defined inner blister.

2. The model

(a) Geometry

We study the equilibrium configurations of two naturally straight inextensible and unshearable Kirchhoff elastic rods of fixed length in the plane (following the general set-up and notation of [10]). The rods are closed into a ring and the longer ring sits inside the shorter one as shown in Figure 2. In the following, the superscripts plus and minus refer to the external and internal loop, respectively. For instance, the length of the two rings are L^+ and L^- but we use $L^\pm$ to denote both. A point $p^\pm$ on the external/internal curve can be parametrized by its Cartesian coordinates

$$\mathbf{r}^\pm(s^\pm) = [x^\pm(s^\pm), y^\pm(s^\pm)], \tag{2.1}$$

where $s^\pm$ represents the arc length. The inextensibilty constraint imposes $(\mathbf{r}^\pm)_{,s^\pm} = \mathbf{t}^\pm$, where $\mathbf{t}^\pm$ are the tangents to their each curve and the subscript represents the differentiation with respect to the arc length, so that

$$x^\pm_{,s^\pm} := \frac{\mathrm{d}x}{\mathrm{d}s^\pm} = \cos(\psi^\pm), \qquad y^\pm_{,s^\pm} := \frac{\mathrm{d}y}{\mathrm{d}s^\pm} = \sin(\psi^\pm), \tag{2.2}$$

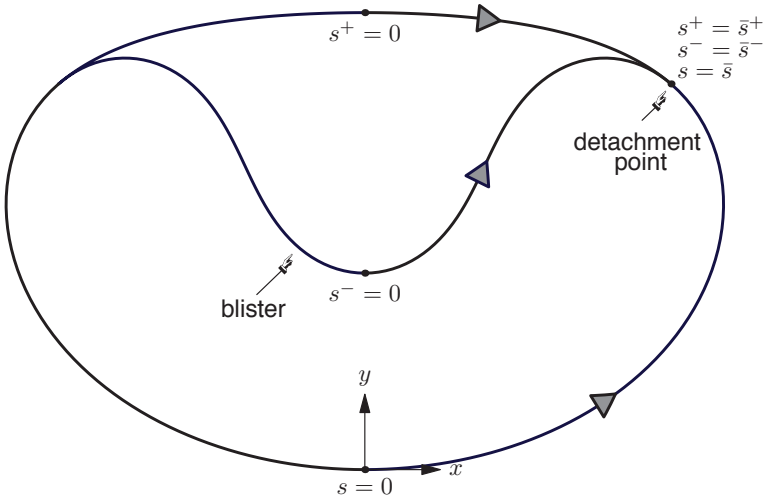

Figure 2. Schematic representation of the equilibrium configuration.

and $\psi^{\pm}$ is the deflection angle with respect to the horizontal axis.

A *blister* is a depression of the inner loop. We look for symmetric configurations so that we set $s^- = 0$ at the vertex of the internal blister, while we have $s^+ = 0$ at the top of the external curve. The detached region for the internal (external) ring falls in the interval $s^- \in [0, \bar{s}^-]$ ($s^+ \in [0, \bar{s}^+]$). To describe the contact region, we introduce

$$\sigma^{\pm} := L^{\pm}/2 - s^{\pm}. \tag{2.3}$$

Since the rings are now in contact with each other, this part of curve can be described by the common arc length

$$s := \sigma^+ = \sigma^-, \quad s \in [0, \bar{s}], \tag{2.4}$$

and by the deflection angle

$$\psi(s) := \psi^+(\sigma^+) = \psi^-(\sigma^-), \quad s \in [0, \bar{s}]. \tag{2.5}$$

In this region $\mathbf{r}(s) := [x(s), y(s)]$ and the inextensibility constraint becomes $\mathbf{r}_{,s} = \mathbf{t}$, where $\mathbf{t}$ is the tangent vector $\mathbf{t} = [\cos(\psi), \sin(\psi)]$; thus, we have

$$x_{,s} = \cos(\psi), \qquad y_{,s} = \sin(\psi). \tag{2.6}$$

(b) Variational formulation

We assume that the two rings are in adhesive contact and subject to internal pressure. For this type of problems with non-trivial boundary conditions, it is therefore easier to formulate equilibrium equations in terms of the critical points of a Lagrangian functional that describes the total energy of the system together with the three inextensibility constraints discussed above:

$$W = \int_0^{\bar{s}} w(\mathbf{r}_{,s}, \mathbf{r}, \psi_{,s}, \psi)\mathrm{d}s + \int_0^{\bar{s}^+} w^+(\mathbf{r}^+_{,s^+}, \mathbf{r}^+, \psi^+_{,s^+}, \psi^+)\mathrm{d}s^+ + \int_0^{\bar{s}^-} w^-(\mathbf{r}^-_{,s^-}, \mathbf{r}^-, \psi^-_{,s^-}, \psi^-)\mathrm{d}s^-. \tag{2.7}$$

First, we consider the Lagrangian density in the detached zone. It consists of three terms: the bending energy density, the density of work done by the distributed external force $\mathbf{b}^{\pm}$, and the

constraint term

$$w^{\pm} = \underbrace{\frac{k^{\pm}}{2}\left(\psi^{\pm}_{,s^{\pm}}\right)^2}_{\text{bending}} \quad \underbrace{-\mathbf{b}^{\pm}\cdot\mathbf{r}^{\pm}}_{\text{work}} \quad \underbrace{-\mathbf{n}^{\pm}\cdot(\mathbf{r}^{\pm}_{,s^{\pm}} - \mathbf{t}^{\pm})}_{\text{constraint}}; \tag{2.8}$$

where $k^{\pm}$ denote the bending rigidities and $\mathbf{n}^{\pm}$ are the vectors of Lagrange multipliers related to the inextensibility constraint.

Second, in the contact region, we include an extra term to model the effect of the capillary adhesion, so that

$$w = \frac{k}{2}\left(\psi_{,s}\right)^2 - \mathbf{b}\cdot\mathbf{r} + \mathbf{n}\cdot(\mathbf{r}_{,s} - \mathbf{t}) - \Delta\gamma; \tag{2.9}$$

where $\Delta\gamma > 0$ denotes the sheets adhesion energy density (per unit length) and $k = k^{+} + k^{-}$.

The first variation of W is obtained by assuming that the curve undergoes an infinitesimal virtual deformation

$$\mathbf{r}^{*} = \mathbf{r} + \epsilon\mathbf{u}, \qquad (\mathbf{r}^{\pm})^{*} = \mathbf{r}^{\pm} + \epsilon\mathbf{u}^{\pm}, \tag{2.10}$$

$$\psi^{*} = \psi + \epsilon\phi, \qquad (\psi^{\pm})^{*} = \psi^{\pm} + \epsilon\phi^{\pm}, \tag{2.11}$$

$$\bar{s}^{*} = \bar{s} + \epsilon\delta\bar{s}, \qquad (\bar{s}^{\pm})^{*} = \bar{s}^{\pm} + \epsilon\delta\bar{s}^{\pm}, \tag{2.12}$$

where ϵ is a small positive parameter. The first variation of W is

$$\begin{aligned}
\delta W \quad = \quad & \int_0^{\bar{s}} [-(\mathbf{n}_{,s} + \mathbf{b})\cdot\mathbf{u} - (k\psi_{,ss} - n_x\sin\psi + n_y\cos\psi)\phi]\mathrm{d}s \\
& + \mathbf{n}(\bar{s})\cdot\mathbf{u}(\bar{s}) - \mathbf{n}(0)\cdot\mathbf{u}(0) + k\psi_{,s}(\bar{s})\phi(\bar{s}) - k\psi_{,s}(0)\phi(0) \\
& + \int_0^{\bar{s}^{+}} [-(\mathbf{n}^{+}_{,s^{+}} + \mathbf{b}^{+})\cdot\mathbf{u}^{+} - (k^{+}\psi^{+}_{,s^{+}s^{+}} - n^{+}_{x}\sin\psi^{+} + n^{+}_{y}\cos\psi^{+})\phi^{+}]\mathrm{d}s^{+} \\
& + \mathbf{n}^{+}(\bar{s}^{+})\cdot\mathbf{u}^{+}(\bar{s}^{+}) - \mathbf{n}^{+}(0)\cdot\mathbf{u}^{+}(0) + k^{+}\psi^{+}_{,s^{+}}(\bar{s}^{+})\phi^{+}(\bar{s}^{+}) - k^{+}\psi^{+}_{,s^{+}}(0)\phi^{+}(0) \\
& + \int_0^{\bar{s}^{-}} [-(\mathbf{n}^{-}_{,s^{-}} + \mathbf{b}^{-})\cdot\mathbf{u}^{-} - (k^{-}\psi^{-}_{,s^{-}s^{-}} - n^{-}_{x}\sin\psi^{-} + n^{-}_{y}\cos\psi^{-})\phi^{-}]\mathrm{d}s^{-} \\
& + \mathbf{n}^{-}(\bar{s}^{-})\cdot\mathbf{u}^{-}(\bar{s}^{-}) - \mathbf{n}^{-}(0)\cdot\mathbf{u}^{-}(0) + k^{-}\psi^{-}_{,s^{-}}(\bar{s}^{-})\phi^{-}(\bar{s}^{-}) - k^{-}\psi^{-}_{,s^{-}}(0)\phi^{-}(0) \\
& + w\delta\bar{s} + w^{+}\delta\bar{s}^{+} + w^{-}\delta\bar{s}^{-}
\end{aligned} \tag{2.13}$$

Taking into account the arbitrariness of $\mathbf{u}(s), \mathbf{u}^{\pm}(s^{\pm}), \phi(s)$ and $\phi^{\pm}(s^{\pm})$, we obtain the Euler-Lagrange equations

$$\mathbf{n}_{,s} + \mathbf{b} = \mathbf{0}, \qquad k\psi_{,ss} - n_x\sin\psi + n_y\cos\psi = 0, \qquad s\in[0,\bar{s}], \tag{2.14a}$$

$$\mathbf{n}^{\pm}_{,s^{\pm}} + \mathbf{b}^{\pm} = \mathbf{0}, \qquad k^{\pm}\psi^{\pm}_{,s^{\pm}s^{\pm}} - n^{\pm}_{x}\sin\psi^{\pm} + n^{\pm}_{y}\cos\psi^{\pm} = 0, \qquad s^{\pm}\in[0,\bar{s}^{\pm}]. \tag{2.14b}$$

We note that in the absence of body forces, the resultant forces $\mathbf{n}$ and $\mathbf{n}^{\pm}$ are constant. Then the problem consists in solving three uncoupled integrable second-order equations (formally equivalent to the classical pendulum equation). Next we compute the boundary conditions. Since the inflection angles are imposed on the symmetry axis, we have $\phi(0) = \phi^{\pm}(0) = 0$. Furthermore, we observe that $\mathbf{u}(0) = \mathbf{0}$, $u_x = u^{\pm}_{x} = 0$, whilst $u^{\pm}_{y}(0)$ are arbitrary, so that

$$n^{\pm}_{y}(0) = 0. \tag{2.15}$$

Concerning the conditions at the detachment point, we first observe that the variations $\mathbf{u}(\bar{s})$, $\mathbf{u}^{\pm}(\bar{s}^{\pm})$, $\phi(\bar{s})$ and $\phi^{\pm}(\bar{s}^{\pm})$ can be written as follows

$$\mathbf{u}(\bar{s}) = \delta\mathbf{r}(\bar{s}) - \mathbf{t}(\bar{s})\delta\bar{s}, \qquad \mathbf{u}^{\pm}(\bar{s}) = \delta\mathbf{r}^{\pm}(\bar{s}^{\pm}) - \mathbf{t}^{\pm}(\bar{s}^{\pm})\delta\bar{s}^{\pm}, \tag{2.16a}$$

$$\phi(\bar{s}) = \delta\psi(\bar{s}) - \psi_{,s}(\bar{s})\delta\bar{s}, \qquad \phi^{\pm}(\bar{s}) = \delta\psi^{\pm}(\bar{s}^{\pm}) - \psi^{\pm}_{,s}(\bar{s}^{\pm})\delta\bar{s}^{\pm}. \tag{2.16b}$$

To assure the continuity of the curves and their curvatures at the detachment point, the following continuity conditions must hold:

$$\mathbf{r}(\bar{s}) = \mathbf{r}^{\pm}(\bar{s}^{\pm}), \qquad \psi(\bar{s}) = \pi + \psi^{\pm}(\bar{s}), \tag{2.17}$$

These last relations, together with the conditions (2.3) lead to

$$\delta\mathbf{r}(\bar{s}) = \delta\mathbf{r}^{+}(\bar{s}^{+}) = \delta\mathbf{r}^{-}(\bar{s}^{-}), \tag{2.18a}$$

$$\delta\psi(\bar{s}) = \delta\psi^{+}(\bar{s}^{+}) = \delta\psi^{-}(\bar{s}^{-}), \tag{2.18b}$$

$$\delta\bar{s} = -\delta\bar{s}^{+} = -\delta\bar{s}^{-}. \tag{2.18c}$$

We can now use (2.16) and (2.18) to write the variations at the detachment point in terms of $\delta\mathbf{r}(\bar{s})$, $\delta\psi(\bar{s})$, δs. By requiring the arbitrariness of these fields, we obtain the Weierstrass-Erdmann corner conditions [11]

$$\mathbf{n}(\bar{s}) + \mathbf{n}^{+}(\bar{s}^{+}) + \mathbf{n}^{-}(\bar{s}^{-}) = \mathbf{0}, \tag{2.19a}$$

$$k\psi_{,s}(\bar{s}) + k^{+}\psi^{+}_{,s^{+}}(\bar{s}^{+}) + k^{-}\psi^{-}_{,s^{-}}(\bar{s}^{-}) = 0, \tag{2.19b}$$

$$\begin{aligned}\left[-k(\psi_{,s})^2 - \mathbf{n}\cdot\mathbf{t} + w\right]_{s=\bar{s}} - \left[-k^{+}(\psi^{+}_{,s^{+}})^2 - \mathbf{n}^{+}\cdot\mathbf{t}^{+} + w^{+}\right]_{s^{+}=\bar{s}^{+}} \\ - \left[-k^{-}(\psi^{-}_{,s^{-}})^2 - \mathbf{n}^{-}\cdot\mathbf{t}^{-} + w^{-}\right]_{s^{-}=\bar{s}^{-}} = 0.\end{aligned} \tag{2.19c}$$

Physically, the first two conditions can be understood as the balance of forces and moments at the points where the three curves meet. The third condition is less trivial and has no direct interpretation in terms of classical mechanical forces. Various forms of this last boundary condition can be found in the literature under different names. In particular, it is derived in O'Reilly's book [12] and in Bigoni's work [9] by using the notions of material momentum and configurational forces (see also [13] where it is called the *adhesion boundary condition*).

3. Analysis

(a) The case with no adhesion and no pressure

We start with the simple case where we assume no adhesion, $\Delta\gamma = 0$, and no external forces, $\mathbf{b} = \mathbf{b}^{\pm} = \mathbf{0}$. As mentioned, it follows that the internal forces $\mathbf{n}(s)$ and $\mathbf{n}^{\pm}(s^{\pm})$ are constant. Furthermore, the boundary conditions (2.15) lead to $n_y^{\pm}(s^{\pm}) = 0$, that, together with (2.19*a*), yield $n_y(s) = 0$.

Equations (2.2), (2.6), and (2.14*b*) then reduce to

$$k\psi_{,ss} - n_x \sin\psi = 0, \qquad s \in [0, \bar{s}], \tag{3.1a}$$

$$[x_{,s}, y_{,s}] = [\cos(\psi), \sin(\psi)], \qquad s \in [0, \bar{s}], \tag{3.1b}$$

$$k^{\pm}\psi^{\pm}_{,s^{\pm}s^{\pm}} - n_x^{\pm}\sin\psi^{\pm} = 0, \qquad s^{\pm} \in [0, \bar{s}^{\pm}], \tag{3.1c}$$

$$[x^{\pm}_{,s^{\pm}}, y^{\pm}_{,s^{\pm}}] = [\cos(\psi^{\pm}), \sin(\psi^{\pm})], \quad s^{\pm} \in [0, \bar{s}^{\pm}], \tag{3.1d}$$

with boundary conditions:

$$x(0) = x^{\pm}(0) = y(0) = \psi(0) = \psi^{\pm}(0) = 0, \tag{3.2a}$$

$$[x(\bar{s}), y(\bar{s})] = [x^{\pm}(\bar{s}^{\pm}), y^{\pm}(\bar{s}^{\pm})], \tag{3.2b}$$

$$\psi(\bar{s}) = \pi + \psi^{\pm}(\bar{s}^{\pm}), \tag{3.2c}$$

$$\psi_{,s}(\bar{s}) = -\psi^{+}_{,s^{+}}(\bar{s}^{+}), \tag{3.2d}$$

$$\psi_{,s}(\bar{s}) = -\psi^{-}_{,s^{-}}(\bar{s}^{-}). \tag{3.2e}$$

and an extra condition on the resultant force

$$n_x = -n_x^+ - n_x^- . \tag{3.3}$$

We treat separately the integration of these equations in the three domains before we match them with the boundary conditions.

(i) The blister

Since the inner loop is in compression, we set $h^- := -n_x^-/k^- > 0$, and consequently Eqn (3.1*c*) becomes, through the well-known Kirchhoff analogy [14], formally equivalent to the pendulum equation

$$(\psi^-)'' + h^- \sin\psi^- = 0, \tag{3.4}$$

where a prime denotes differentiation with respect to s^-. The inflection angle $\psi^-(s^-)$ starts at zero. It is therefore an increasing function up to $s_0^- \in (0, \bar{s}^-)$ where we define $\psi_0^- := \psi^-(s_0^-)$ and $\bar{\psi}^- := \psi^-(\bar{s}^-)$. Equation (3.4) admits the first integral

$$\frac{1}{2}[(\psi^-)']^2 - h^- \cos(\psi^-) = -h^- \cos(\psi_0^-), \tag{3.5}$$

whence

$$(\psi^-)' = \pm\sqrt{2h^-[\cos(\psi^-) - \cos(\psi_0^-)]}, \tag{3.6}$$

with

$$h^- = \frac{(\lambda^-)^2}{2[\cos(\bar{\psi}^-) - \cos(\psi_0^-)]}, \qquad \lambda^- := (\bar{\psi}^-)'(\bar{s}^-). \tag{3.7}$$

Since $(\psi^-)' > 0$ for $s^- \in (0, s_0^-)$ and $(\psi^-)' < 0$ for $s^- \in (s_0^-, \bar{s}^-)$, we can integrate (3.6) to obtain

$$\bar{s}^- = \frac{1}{\sqrt{2h^-}}\left[\int_0^{\psi_0^-} \frac{\mathrm{d}\psi^-}{\sqrt{\cos(\psi^-) - \cos(\psi_0^-)}} - \int_{\psi_0^-}^{\bar{\psi}^-} \frac{\mathrm{d}\psi^-}{\sqrt{\cos(\psi^-) - \cos(\psi_0^-)}}\right]. \tag{3.8}$$

By using the restrictions $0 < \psi_0^- < \pi/2$ and $|\bar{\psi}^-| < |\psi_0^-|$, we can rewrite (3.8) in terms of elliptic integrals:

$$\bar{s}^- = \sqrt{\frac{2}{h^-(1 - \cos(\psi_0^-))}}\,[2\mathrm{F}(q_0) - \mathrm{F}(\bar{q})]\,, \tag{3.9}$$

where $\mathrm{F}(\cdot)$ denotes the incomplete elliptic integral (see [15]) of the first kind and

$$q_0 := \left[\frac{\psi_0^-}{2}, \csc^2\left(\frac{\psi_0^-}{2}\right)\right], \qquad \bar{q} := \left[\frac{\bar{\psi}^-}{2}, \csc^2\left(\frac{\psi_0^-}{2}\right)\right]. \tag{3.10}$$

By exploiting the same technique, we can integrate Equation (2.2) to obtain:

$$\bar{x}^- = \sqrt{\frac{2(1 - \cos(\psi_0^-))}{h^-}}[-2\mathrm{E}(q_0) + \mathrm{E}(\bar{q})] + \bar{s}^- \cos(\psi_0^-), \tag{3.11}$$

where $\mathrm{E}(\cdot)$ denotes the incomplete elliptic integral of the second kind.

(ii) The outer detached curve

Since the outer curve is in tension, we set $h^+ := -T^+/k^+ < 0$. Then Equation (3.1*c*) becomes

$$(\psi^+)'' + h^+ \sin(\psi^+) = 0, \tag{3.12}$$

where prime denotes now differentiation with respect to s^+. Equation (3.12) admits the first integral

$$\frac{1}{2}[(\psi^+)']^2 - h^+ \cos(\psi^+) = c^+, \tag{3.13}$$

with $c^+ + h^+ \cos(\psi^+) > 0$. We set $\bar{\psi}^+ := \psi^+(\bar{s}^+)$. In the domain $s^+ \in [0, \bar{s}^+]$, $\psi(s^+)$ monotonically decreases, so that

$$\bar{s}^+ = -\int_0^{\bar{\psi}^+} \frac{\mathrm{d}\psi^+}{\sqrt{2[c^+ + h^+ \cos(\psi^+)]}} = -\frac{\sqrt{2}\mathrm{F}(\bar{\mathcal{Q}}^+)}{\sqrt{c^+ + h^+}}, \tag{3.14}$$

where

$$\bar{\mathcal{Q}}^+ := \left[\frac{\bar{\psi}^+}{2}, \frac{2h^+}{c^+ + h^+}\right].$$

In a similar way, we obtain

$$\bar{x}^+ = -\frac{\sqrt{2(c^+ + h^+)}}{h^+}\mathrm{E}(\bar{\mathcal{Q}}^+) - \frac{c^+}{h^+}\bar{s}^+. \tag{3.15}$$

(iii) The contact region

We solve the pendulum equation

$$\psi'' + h \sin(\psi) = 0, \tag{3.16}$$

where prime denotes a derivative with respect to s and where $h := -n_x/k$ is an unknown constant. The first integral of (3.16) is

$$\frac{1}{2}[(\psi)']^2 - h \cos(\psi) = c, \tag{3.17}$$

where $c + h\cos(\psi) > 0$. Let $\bar{s}$ and $\bar{\psi} := \psi(\bar{s})$ be the arc length and deflection angle at the detachment point. We assume that in the region $s \in [0, \bar{s}]$, $\psi(s)$ monotonically increases, so that

$$\bar{s} = \int_0^{\bar{\psi}} \frac{\mathrm{d}\psi}{\sqrt{2[c + h\cos(\psi)]}} = \frac{\sqrt{2}\mathrm{F}(\bar{\mathcal{Q}})}{\sqrt{c+h}}. \tag{3.18}$$

Finally, integration of Equation $(2.6)_1$ gives

$$\bar{x} = \frac{\sqrt{2(c+h)}}{h}\mathrm{E}(\bar{\mathcal{Q}}) - \frac{c}{h}\bar{s}, \tag{3.19}$$

with

$$\bar{\mathcal{Q}} := \left[\frac{\bar{\psi}}{2}, \frac{2h}{c+h}\right].$$

(iv) Discussion

We are interested in computing the shape as a function of the two dimensionless parameters

$$\mu := \frac{L^-}{L^+}, \qquad \kappa := \frac{k^+}{k^-}. \tag{3.20}$$

The parameter μ increases as the inner loop increases in length with an inner loop of fixed length. An increase in κ represents a (relative) stiffening of the outer loop.

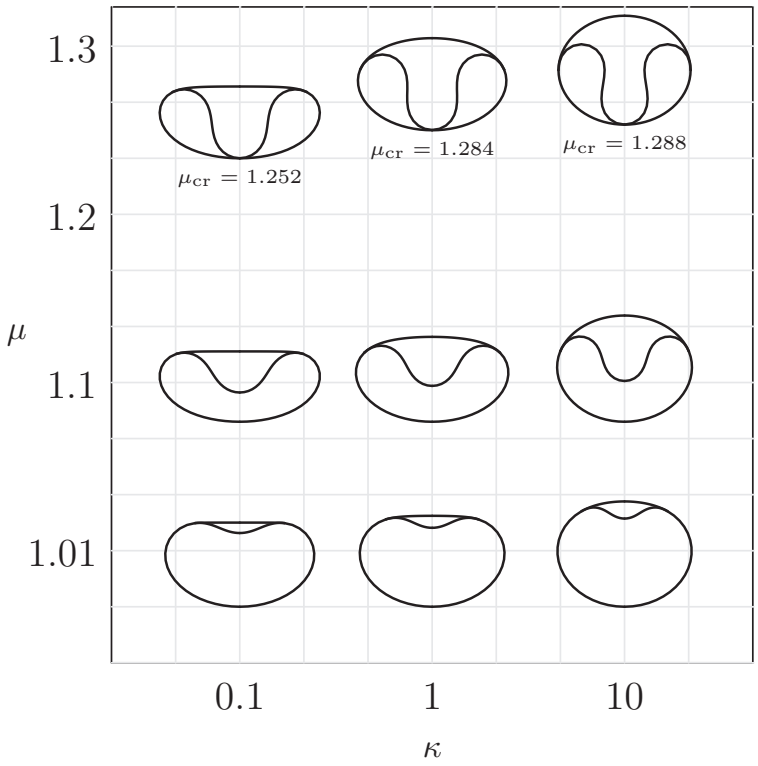

Figure 3. Equilibrium configurations for several values of κ and μ. The values of μ for the upper row are indicated on the figure and the two lower rows correspond to $\mu = 1.1$ and 1.01.

For fixed values of ν and κ, the solutions can be obtained by determining the constants appearing in the expressions for each segments. By using the first integrals (3.5), (3.13) and (3.17) together with the conditions (3.2*e*), we obtain

$$c + h\cos(\bar{\psi}) = c^+ + h^+\cos(\bar{\psi}^+), \tag{3.21}$$

$$c + h\cos(\bar{\psi}) = h^-[\cos(\bar{\psi}^-) - \cos(\psi_0^-)]. \tag{3.22}$$

Equation (3.3) implies

$$h = -\frac{k^+h^+ + k^-h^-}{k}. \tag{3.23}$$

Altogether, we have 9 equations at disposal to compute the nine unknowns $\bar{\psi}$, $\bar{\psi}^+$, $\bar{\psi}^-$, c, c^+, ψ_0^-, h, h^+, and h^-. However, Equations (3.2*c*)$_2$, (3.21), (3.22) and (3.23) are used to eliminate $\bar{\psi}$, $\bar{\psi}^-$, c, c^+, and h, so that we only have the four unknowns to ψ_0^-, $\bar{\psi}^+$, h^+, h^- that can be determined by solving numerically Equations (3.2*c*)$_1$, (2.3) using the expressions for $\bar{s}$, $\bar{s}^\pm$, $\bar{x}$ and $\bar{x}^\pm$ obtained above.

Once these constants have been determined, the three functions $\psi^\pm$ and ψ are fully specified and Equations (2.2) and (2.6) are used to compute the equilibrium shapes for given μ and κ.

In Figures 3 we show different equilibrium shapes as these two parameters are varied. As expected, when the outer ring is stiff, it is almost circular and we recover the solutions for the rigid ring described before [3,4]. When the outer ring is soft, it flattens as the the inner ring buckles.

As length increase, equilibrium shapes are computed up to $\mu_{\rm cr}$ that corresponds to a *triple contact* between the blister and the outer ring. Remarkably, this contact occurs for values of μ in a small range: between 1.2 and 1.3 with the rigid case being obtained around $\mu \approx 1.288$. For $\mu > \mu_{\rm cr}$,

a second continuous region of contact is established and an extra interval in arc length for that zone should be introduced to compute the new solution.

It is important to note that in the limit of an extremely soft external ring ($\kappa \ll 1$) the assumption of inextensibility may not be valid for a regular elastic material. Indeed, for a small length difference and a soft external ring, it will become energetically advantageous to stretch the outer ring rather than buckle the inner one. In this case, both rings would remain circular and we expect a transition for small κ between a stretched-circular solution to a solution with a buckling-dominated blister solution.

(b) The role of adhesion

Next, we consider the influence of the capillary adhesion $\Delta\gamma > 0$. In this case, the Euler-Lagrange equations (3.1*a*) and (3.1*c*) remain unchanged. The same is true for the boundary conditions (3.2*b*) and the contact condition on the internal force (3.3). Capillary adhesion enters into Equations (2.19*b*) and (2.19*c*) and leads to the following conditions on the curvature at the detachment point:

$$\left[\psi^{+}_{,s^+}(\bar{s}^+) + \psi_{,s}(\bar{s})\right]^2 = \frac{k^-}{k^+}\frac{2\Delta\gamma}{k}, \tag{3.24a}$$

$$\left[\psi^{-}_{,s^-}(\bar{s}^-) + \psi_{,s}(\bar{s})\right]^2 = \frac{k^+}{k^-}\frac{2\Delta\gamma}{k}, \tag{3.24b}$$

that replace Equations (3.2*e*). We verify that in the absence of capillary adhesion, Equations (3.24) reduce to (3.2*e*). Thus, the effect of capillary adhesion only appears in the boundary conditions and the problem is still integrable. Therefore, we use the method from the previous section to obtain closed-form solutions.

In the presence of adhesion we introduce the dimensionless *gluing number*

$$\eta := \frac{L^+}{2\pi}\sqrt{\frac{\Delta\gamma}{k^-}}, \tag{3.25}$$

that measures the relative adhesion strength compared to the stiffness of the material. When μ and κ are fixed, increasing gluing favors the growth of the contact region.

Large enough adhesion creates a new possibility of self-contact for the inner ring where it can come in contact with itself in an intermediate point on the symmetry axis, creating self-encapsulation [8,9].

Figure 4 sketches the critical curve in the parameter plane η–μ where the blister comes first in contact, either with the inner ring (small η) or with itself (large η). The maximum of the curve corresponds to inner curves that touch exactly the inner ring and itself at the same time.

(c) The role of internal pressure

Next, we consider the effect of a pressure P (measured here as a force per unit length) inside the inner ring, while we assume that both the external pressure and the pressure between the two rings vanish identically. Pressure is introduced in the system through the body force. In our case, the density of external force is orthogonal to the rings so that:

$$\mathbf{b} = P(\sin\psi, -\cos\psi), \tag{3.26a}$$

$$\mathbf{b}^+ = \mathbf{0} \tag{3.26b}$$

$$\mathbf{b}^- = P(\sin\psi^-, -\cos\psi^-). \tag{3.26c}$$

The presence of P introduce a new dimensionless parameter in the problem, the *dimensionless pressure*:

$$p := -\frac{Pr^3}{k}, \tag{3.27}$$

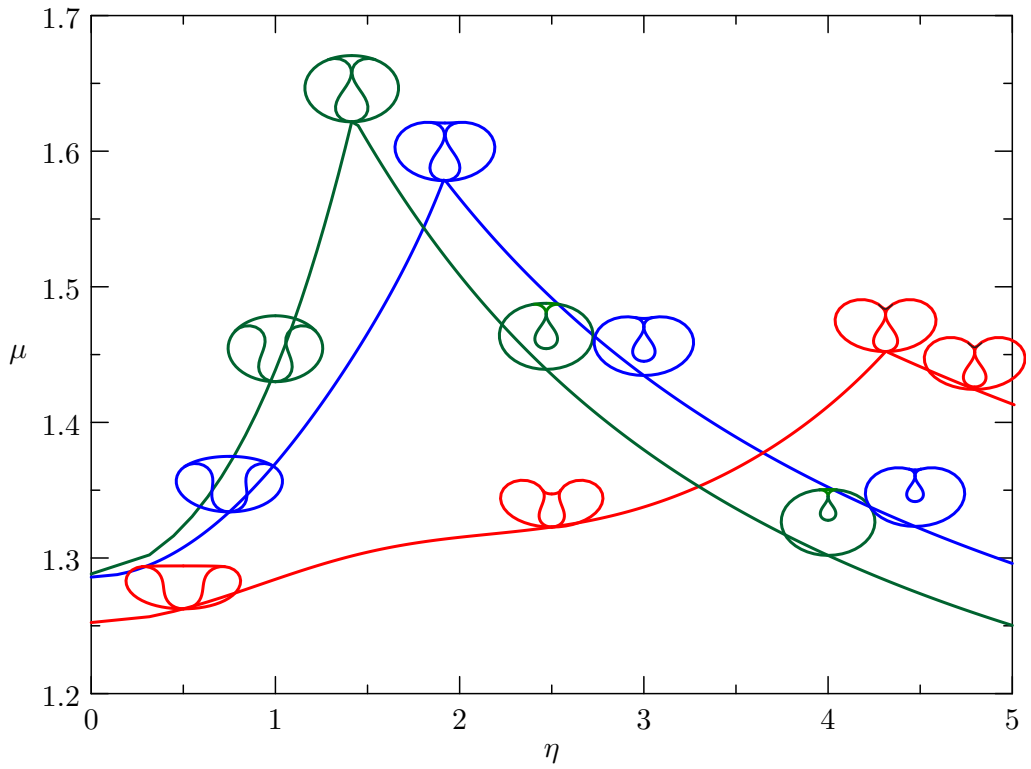

Figure 4. . Critical values of the length ratio μ at which the self-contact occurs as a function of the gluing number η, for $\kappa = 0.1$ (red) (note that we have added a small black curves on the two red rings for large η to show the position where the outer ring is not in contact with the inner ring), $\kappa = 1$ (blue) and $\kappa = 10$ (green).

where a positive value of p corresponds to a negative internal pressure sucking the ring inward.

We study the equilibrium shapes of two rings with the same length $\mu = 1$, with no capillary adhesion $\Delta\gamma = 0$. Two completely adhered circular rings are a trivial solution of the equilibrium equations. This solution exist for any values of P. However, the analysis of the linearized equations around the circular solution, shows that when a sufficiently strong negative pressure is applied the circular solution undergoes a distortion. The critical threshold correspond to the classical problem of an elastic ring under pressure [16] and is given by $p_{\rm cr} = 3$. Beyond this critical value, the two rings are deformed while remaining glued to each other. However, the inner ring can also detach and form a blister. Therefore, we need to compare the competition between three different solutions: (i) the circular solution, (ii) the deformed rings with no blister and (iii) the deformed rings with a blister.

The nature of this phase transition and the shape at the critical point depends on the parameter κ. To establish the influence of κ on the critical threshold, we compute the energy landscape, by drawing the dimensionless energy $\epsilon := Wr/k$ (being r the radius of the rings) as a function of p, for the three solutions (see Figure 5).

Circular solutions: By using Equation (3.26), together with Equations (2.9), (2.8) and (2.7), we deduce with the aid of the divergence theorem that pressure potential is $-PA$, where A is the area bounded by the internal ring. Thus, the dimensionless energy of the circular solution is

$$\epsilon_{\rm circ} = \pi(1 + p).$$

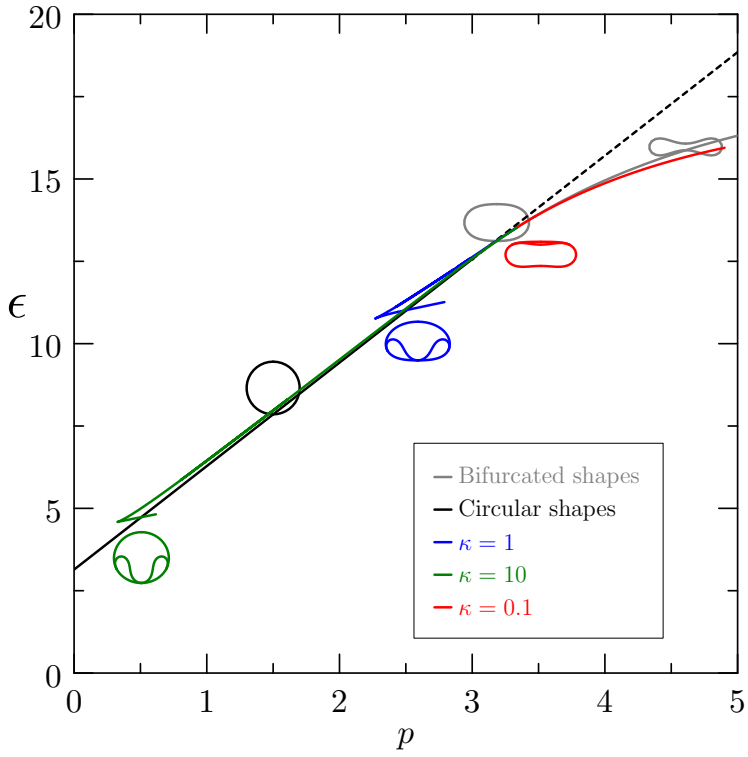

Figure 5. . Energy landscape. Representation of the total energy as function of the dimensionless pressure. The red, blue and green insets represent the shapes at the critical points for $\kappa = 0.1$, $\kappa = 1$ and $\kappa = 10$, respectively.

Deformed solutions without blister: This branch exists only for $p > p_{\rm cr}$. For these configurations $\bar{s} = \pi r$, while $\bar{s}^+$ and $\bar{s}^-$ vanish identically. Thus the total energy takes the simplified form:

$$W_{\rm adh} = \frac{k}{2}\int_0^{\pi r} (\psi_{,s})^2 {\rm d}s - PA. \tag{3.28}$$

The dimensionless energy $\epsilon_{\rm adh}(p) := W_{\rm adh} r/k$ has been computed numerically. The left end of this branch joins the circular branch with continuous derivative. This bifurcation is a second-order phase transition at $p_{\rm cr}$. As established from bifurcation theory, beyond $p_{\rm cr}$ the circular branch becomes locally unstable. Note that neither $\epsilon_{\rm circ}(p)$ nor $\epsilon_{\rm adh}(p)$ depend on κ.

Deformed solutions with blister: The blister solution is strongly influenced by the relative stiffness κ. Consider for instance the case $\kappa = 10$. In this case, past a critical value of p, there are two solutions with blister. The higher energy solution is nearly circular and has an extremely small blister (with high bending energy). The lower energy solution has a larger blister. At the point $p_{10} = 0.507$ (with $\epsilon = 4.733$) this branch intersects the branch corresponding to the circular solution and becomes the absolute minimum for $p > 0.507$. This means, that in an experiment where the pressure decreases (starting from zero) the first transition that takes place is from a circular shape to a shape with a blister. Since at that time the blister is already of finite size, this is a first-order phase transition: as the pressure crosses the critical threshold the blister develops suddenly. The green insets represents at the shape at the critical point.

The same behavior is observed for various values of $\kappa \geq 1$ with a bifurcation from circular shapes to solutions with blister. However, for $\kappa = 0.1$, we observe that the solution with a blister only appears for values of $p_1 > p_{\rm cr}$. Then, the lower energy branch corresponds to a small blister

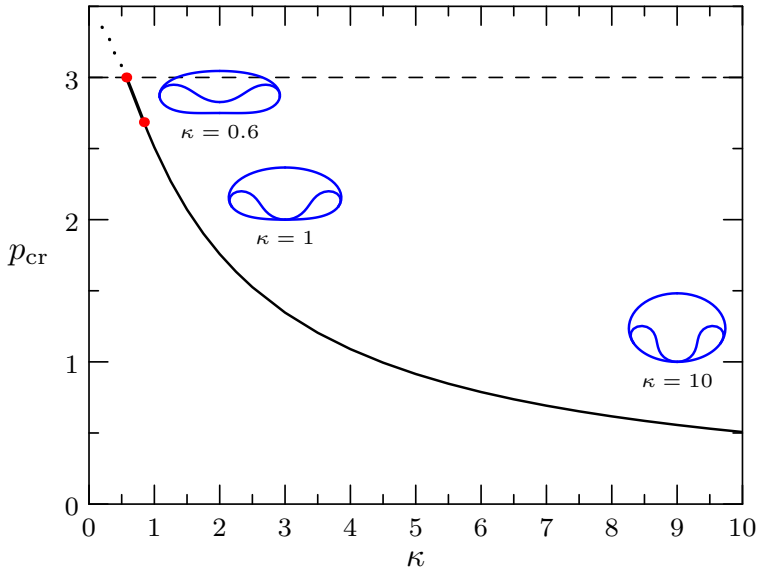

Figure 6. Critical threshold as function of κ, For $0 < \kappa \lesssim 0.57$, the circular solution buckles into non circular shapes (without blister) at $p = 3$ (dashed curve) and subsequently, at $p > 3$, a blister forms (dotted curve). For $\kappa \gtrsim 0.57$ (solid curve), the circular solution becomes energetically more expensive than a blistered solution which appears with finite size without self-contact (tract of curve between the two red dots) or with a point of self-contact. The insets show typical shapes at the transition.

that develops continuously on the deformed shape, another second-order phase transition. So, for $\kappa = 0.1$, as p increases from zero, the first bifurcation occurs at $p_{\rm cr}$ and a second bifurcation at p_1.

We can now study these bifurcations as a function of κ as shown in Figure 6. We distinguish the following cases:

(i) For $0 < \kappa \lesssim 0.57$, the first (second-order) transition occurs at $p_{\rm cr} = 3$ from circular to deformed without blister. A second (second-order) transition occurs at $p_\kappa > 3$ at which a blister forms.

(ii) For $0.57 \lesssim \kappa \lesssim 0.84$: a first-order transition takes place at $p_\kappa < 3$ where the solution switches from circular to blistered without self-contact.

(iii) For $\kappa \gtrsim 0.84$: the solution switches from circular to blistered with a single point of self-contact at the bottom of ring at the transition.

4. Conclusions

The problem of two nested elastic rings in contact is an ideal playground to explore problems of self-contact in rods. We have favoured a variational formulation of the problem since it provides directly the boundary conditions associated with a moving contact point. These boundary conditions cannot be easily obtained within a traditional framework of force balance. Owing to the integrability of isotropic rods, the analysis of this problem can be done exactly in terms of elliptic functions and the shape is found by solving a set of coupled transcendental equations for the 5 arbitrary constants. In the absence of adhesion or pressure, the problem is fully specified by two dimensionless parameters (the relative length and stiffness of the two rods). In that case, a blister forms and increases in size with the relative length until a triple contact point is reached at the bottom of the inner ring. In the presence of adhesion, self-encapsulation can occur before the triple contact point. With both internal pressure and adhesion, the problem is richer with

a competition between up to 4 different symmetric solutions. An energy analysis then reveals that different bifurcations can take place as a function of the relative stiffness. However, a more complete study of the equilibrium featured should include the local stability and, hence, the analysis of the second variation of the total energy (see [12,17]).

Ackowledgments: We gladly acknowledge Xiaoyu Luo who introduced us to the problem of arterial dissection that served as the original motivation for this problem and to Tom Mullins and Ousmane Kodio for interesting discussions.

Ethics statement. This work did not involve any active collection of human data.

Data accessibility statement. This work does not have any experimental data.

Competing interests statement. We have no competing interests.

Authors' contributions. All authors contributed equally to the work presented.

Funding statement. This research was not funded.

References

1. Alan C Braverman.
Acute aortic dissection.
Circulation, 122(2):184–188, 2010.
2. Lei Wang, Steven M Roper, Nicholas A Hill, and Xiaoyu Luo.
Propagation of dissection in a residually-stressed artery model.
Biomechanics and modeling in mechanobiology, pages 1–11, 2016.
3. R. De Pascalis, G. Napoli, and S. S. Turzi.
Growth-induced blisters in a circular tube.
Physica D, 283:1–9, 2014.
4. G. Napoli and S. Turzi.
Snap buckling of a confined thin elastic sheet.
Proc. R. Soc. A, 471(2183):20150444, 2015.
5. Jee E Rim, Prashant K Purohit, and William S Klug.
Mechanical collapse of confined fluid membrane vesicles.
Biomech. Model. Mechan., 13(6):1277–1288, 2014.
6. Andrew L Hazel and Tom Mullin.
On the buckling of elastic rings by external confinement.
Phil. Trans. R. Soc. A, 375(2093):20160227, 2017.
7. JB Bostwick, MJ Miksis, and SH Davis.
Elastic membranes in confinement.
Journal of The Royal Society Interface, 13(120):20160408, 2016.
8. Joseph E Flaherty and Joseph B Keller.
Contact problems involving a buckled elastica.
SIAM Journal on Applied Mathematics, 24(2):215–225, 1973.
9. F Bosi, D Misseroni, F Dal Corso, and D Bigoni.
Self-encapsulation, or the 'dripping'of an elastic rod.
In *Proc. R. Soc. A*, volume 471, page 20150195. The Royal Society, 2015.
10. A. Goriely.
The Mathematics and Mechanics of Biological Growth.
Springer Verlag, New York, 2017.
11. I. M. Gelfand and S. V. Fomin.
Calculus of variations.
Prentice Hall, 1963.
12. O. M. O'Reilly.

Modeling Nonlinear Problems in the Mechanics of Strings and Rods: The Role of the Balance Laws. Springer New York, 2016.
13. C. Majidi.
Remarks on formulating an adhesion problem using euler's elastica (draft).
Mech Res Comm, 34(1):85–90, 2007.
14. M. Nizette and A. Goriely.
Towards a classification of Euler-Kirchhoff filaments.
J. Math. Phys., 40:2830–2866, 1999.
15. M. Abramowitz and I. A. Stegun.
Handbook of Mathematical Function with Formulas, Graphs, and Mathematical Tables.
Dover, New York, 1964.
16. I Tadjbakhsh and F Odeh.
Equilibrium states of elastic rings.
Journal of Mathematical Analysis and Applications, 18(1):59–74, 1967.
17. Carmel Majidi, Oliver M. O'Reilly, and John A. Williams.
Bifurcations and instability in the adhesion of intrinsically curved rods.
Mechanics Research Communications, 49:13–16, 2013.